Short communication

Performance of anode-supported solid oxide fuel cell with thin bi-layer electrolyte by pulsed laser deposition

Zigui Lu [a,*], John Hardy [a], Jared Templeton [a], Jeffry Stevenson [a], Daniel Fisher [b], Naijuan Wu [b], Alex Ignatiev [b]

[a] Pacific Northwest National Laboratory, Richland, WA, 99352, USA
[b] Center for Advanced Materials, University of Houston, Houston, TX 77024, USA

ABSTRACT

Anode-supported yttria stabilized zirconia (YSZ)/samaria doped ceria (SDC) bi-layer electrolytes with uniform thickness and high density were fabricated by pulsed laser deposition at 1000 °C. Fuel cells with such bi-layer electrolytes were fabricated and tested, yielding open circuit voltages from 0.94 to 1.0 V at 600–700 °C. Power densities from 0.4 to 1.0 W cm^{-2} at 0.7 V were achieved in air at temperatures of 600–700 °C. Cell performance was improved in flowing oxygen, with an estimated peak power density of over 2 W cm^{-2} at 650 °C, assuming the same overall resistance over the entire range of current density. The high cell performance was attributed to the very low ohmic resistance of the fuel cell, owing to the small thickness of the electrolyte. Stable performance was also demonstrated in that the voltage of the fuel cell showed very little change at a constant current density of 1 A cm^{-2} during more than 400 h of operation at 650 °C in flowing oxygen. SEM analysis of the fuel cell after testing showed that the bi-layer electrolyte had retained its chemical and mechanical integrity.

Published by Elsevier B.V.

1. Introduction

Reducing the operating temperature of solid oxide fuel cells (SOFC) to intermediate temperatures (500–750 °C) offers several advantages, including prolonged cell component lifetimes, slower degradation rates, reduced stack insulation requirements, and use of low-cost stainless steel for interconnects and gas manifolds. To achieve high power densities at these intermediate temperatures, the ohmic and polarization resistances of the fuel cell both need to be kept as low as possible (usually less than 0.2 Ω cm^2 for each). The ohmic resistance of the cell can be reduced by either reducing the thickness of the state-of-the-art electrolyte, Y_2O_3-stabilized ZrO_2 (YSZ), or by using alternative electrolyte materials with higher ionic conductivity, among which, Sm or Gd-doped ceria (SDC or GDC) or Sr and Mg-doped lanthanum gallate (LSGM) have received much attention [1,2]. To achieve low polarization resistance at intermediate temperature, mixed ionic and electronic conductors such as $La_{1-x}Sr_xCo_{1-y}Fe_yO_3$ (LSCF) are intensively investigated to replace the traditional $La_{1-x}Sr_xMnO_3$ (LSM) cathode, which is widely used at 800 °C or higher [3–5]. Mixed ionic and electronic conducting cathode materials show superior performance compared to LSM

because their mixed conductivity extends the reaction zone beyond the interface of the cathode and electrolyte [6,7]. An interlayer such as SDC or GDC is usually applied between the mixed-conducting cathode and the YSZ electrolyte to prevent chemical reactions during cell fabrication and operation [8].

By varying the thickness of the anode-supported YSZ electrolyte, Lu et al. studied the contribution of the YSZ electrolyte to the total ohmic resistance of the anode-supported fuel cell and found that at temperatures no lower than 650 °C, the area specific resistance (ASR) of an 8-μm thick electrolyte is less than 0.1 Ω cm^2, much smaller than the contributions from other cell components to the total ohmic resistance [9]. By improving the density of the SDC interlayer fabricated by pulsed laser deposition, the ohmic resistance of the cell was significantly reduced, leading to an impressive increase in power density [10]. However, the contribution of an 8 μm thick YSZ electrolyte to the total ASR increases from 0.02 to 1 Ω cm^2 as the temperature decreases from 750 to 500 °C. Therefore, the thickness of the YSZ electrolyte needs to be further reduced at low temperatures to retain a low ohmic ASR of 0.2 Ω cm^2. The difficulties associated with fabricating large area, ultra-thin films with uniform thickness and good mechanical stability over long-term operation are major challenges. Recently, fuel cells with bi-layer electrolytes, usually doped ceria layers together with purely ionic conducting layers such as YSZ or stabilized Bi_2O_3, have gained a lot of attention due to their low ohmic resistance and high open circuit voltage (OCV). In this configuration, the ionic conductor layer

blocks the electron conduction, thus preventing internal current leakage, and is kept as thin as possible to minimize the ohmic resistance, while the thick dense ceria layer offers mechanical stability and separates the fuel from air [11–15].

Fabrication of the dense bi-layer electrolyte thin film is very difficult because of the poor sinterability of doped ceria and YSZ at temperatures lower than 1200 °C. Sintering at elevated temperatures is not viable due to the formation of an electrically insulating interface between ceria and YSZ [16,17]. Many attempts have been made to fabricate the dense bi-layer structure through a variety of techniques, including pulsed laser deposition [11–13], screen-printing [14,15], sputtering [18], tape casting [19], and electrophoretic deposition [20], with the peak power densities of the resulting cells ranging widely from 0.25 W cm^{-2} to 1.8 W cm^{-2} at 650 °C. Fabrication methods such as tape casting and electrophoretic deposition, although cost-effective and easy to scale up, require a high sintering temperature to fully densify the electrolyte. Cells fabricated using these techniques usually have high ohmic resistances and, therefore, low peak power densities [19,20]. In this short communication, we report the fabrication and characterization of fuel cells with anode-supported SDC-YSZ bi-layer electrolytes by pulsed laser deposition. The ohmic and polarization resistances of the fuel cell were characterized by electrochemical impedance spectroscopy. More importantly, the stability of the fuel cell with the thin bi-layer electrolyte was also evaluated.

2. Experimental

The YSZ-SDC bi-layer electrolyte was fabricated by pulsed laser deposition (PLD) on a Ni + YSZ anode substrate. The anode substrate consisted of two layers, a porous Ni + YSZ bulk layer and a Ni + YSZ functional layer with thicknesses of 1 mm and 8 μm, respectively. The bi-layer anode substrate was fabricated by a tape casting and lamination process detailed elsewhere [21]. The anode substrate was sintered at 1385 °C for 2 h and creep-flattened at 1350 °C for 2 h. A thin layer of YSZ (700 nm) was deposited on the dense functional anode by PLD at 1000 °C for 30 min at an oxygen partial pressure of 150 mTorr. After the deposition of the YSZ layer, an SDC layer was deposited on top of the YSZ layer under the same conditions for 60 min. Details about the PLD process can be found elsewhere [10,22]. The deposition conditions such as temperature and oxygen partial pressure were chosen based on considerations of film density and deposition rate. Lower oxygen partial pressure generally results in a denser film but at a slower deposition rate, while higher deposition temperature leads to improved density.

La$_{0.6}$Sr$_{0.4}$Co$_{0.2}$Fe$_{0.8}$O$_3$ (LSCF) and La$_{0.8}$Sr$_{0.2}$CoO$_3$ (LSC) were used as the cathode functional layer and cathode current collector, respectively. The as-received LSCF powder (d_{50} = 1.0 μm) was milled down to about 0.3 μm. The LSCF cathode was fabricated by screen-printing LSCF ink onto the electrolyte and sintering at 900 °C for 2 h. LSC was screen-printed onto the LSCF and sintered at 850 °C for 2 h to serve as the cathode current collector. The cathode area of 2 cm^2 was used to calculate the power density and ASR. All of the inks used in this study had about 40% solids loading by weight and were prepared by mixing ceramic powders with V-006 binder (Heraeus) on a three-roll mill. Au mesh and Ni mesh were used to collect current from the cathode and anode, respectively. The cells were sealed to alumina tubes using G18 glass sealant. The cells were heated to 850 °C for 30 min to achieve a good seal and then cooled to the operating temperature at which the anode was reduced. I–V sweep and impedance spectroscopy were performed using a Solartron 1470 Multistat coupled with a Solartron 1255 frequency response analyzer. During testing, hydrogen bubbled through water was supplied to the anode and either dry air or oxygen was supplied to cathode. After testing, the fuel cells
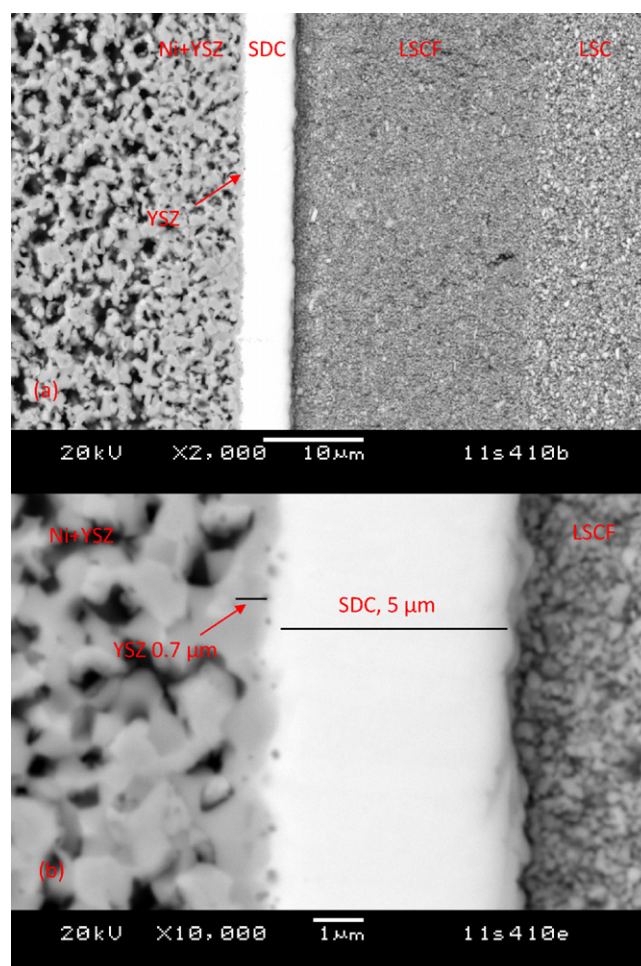

Fig. 1. Cross-sections with magnifications of (a) 2000× and (b) 10,000× of fuel cells with PLD deposited YSZ and SDC electrolytes after testing.

were mounted in epoxy resin and polished for cross-sectional SEM observations (JEOLJSM-5900LV).

3. Results and discussion

The cross-section of a fuel cell with a PLD bi-layer electrolyte after cell testing at 650 °C for over 400 h is shown in Fig. 1. A thin, dense, and continuous YSZ layer with a thickness of 0.5–1.0 μm was deposited on the anode substrate. On top of the thin YSZ layer, an SDC layer about 5 μm thick was in good contact with the YSZ layer except for a few isolated pores. No porosity was detected in either the YSZ or SDC layer after deposition. The pores at the interface will probably cause a slight increase in the ionic resistance of the composite electrolyte simply due to the increase in the effective aspect ratio of the portion of the electrolyte in the vicinity of the YSZ/SDC interface that occurs because of the volume that is occupied by non-conductive pores. However, it is difficult to accurately predict the extent of the increase without knowledge of the resistivity of the material in the interfacial region as a function of distance from the interface together with knowledge of the cross-sectional area of the porosity as a function of distance from the interface. If these things were known, a model based on the equation relating resistance to resistivity, length, and cross-sectional area could be used to estimate the effect of the interfacial porosity on resistance. The LSCF cathode and LSC cathode current collector exhibited very fine microstructures. Particle sizes under 1 μm were observed in the
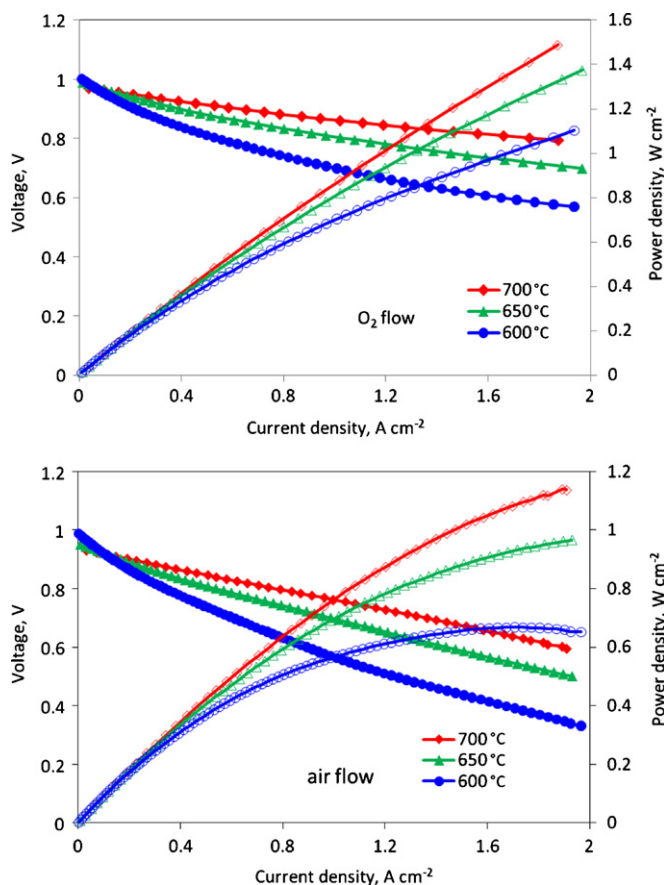
Fig. 2. I–V curves of the fuel cell at various temperatures with flowing oxygen or air on the cathode.

Fig. 3. Electrochemical impedance spectroscopy of the fuel cell at various temperatures with flowing oxygen or air on the cathode.

LSCF cathode. The thicknesses of the LSCF cathode and LSC cathode current collector were about 20 and 30 μm, respectively.

During cell testing, open circuit voltages (OCV) of 0.94, 0.95, and 0.99 V in flowing air and 0.98, 0.99, and 1.00 V in flowing oxygen were observed at temperatures of 700, 650, and 600 °C, respectively. These OCVs are higher than those of the cells with single-layer doped ceria electrolytes, which usually range from 0.7 to 0.9 V in this temperature range, depending on the thickness and density of the electrolyte [23–26]. The higher OCV can be attributed to the addition of the thin YSZ layer which effectively blocks the leakage current through the SDC layer. The OCVs in this study are higher than or comparable to those of cells with similar configurations but are still lower than the theoretical OCV in this temperature range, which means that a slightly thicker YSZ layer might be required to achieve near theoretical OCV [10–15,18].

The I–V curves of the fuel cell in flowing air and oxygen at different temperatures are presented in Fig. 2. Power densities of 0.96, 0.69 and 0.42 W cm^{-2} were achieved at 0.7 V for the fuel cell tested in air at temperatures of 700, 650, and 600 °C, respectively. The peak power densities of the cell under some conditions could not be measured because the test equipment was limited to
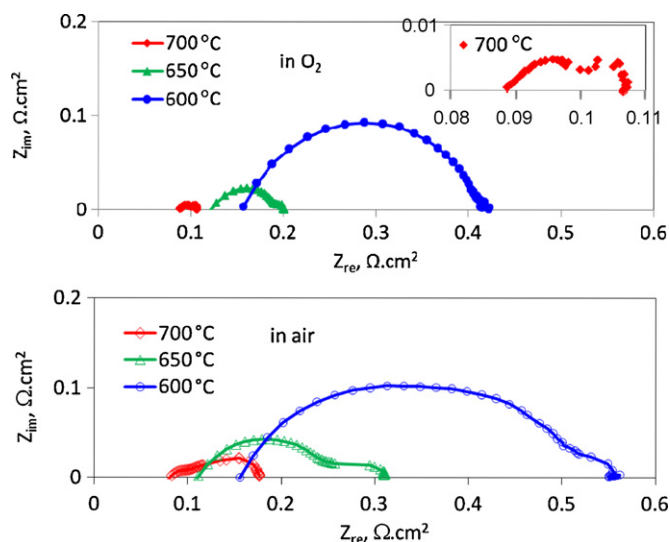
a maximum current of 2 A. The power densities of the cell were significantly improved when tested in flowing oxygen, reaching 1.5 W cm^{-2} at 0.79 V, 1.37 W cm^{-2} at 0.7 V, and 0.7 W cm^{-2} at 0.7 V at temperatures of 700, 650, and 600 °C, respectively. The significant improvement in power density can be attributed to the pronounced decrease in polarization resistance, shown in the electrochemical impedance spectra of the cell (Fig. 3), as well as to the slight increase in OCV. From the impedance spectra, ohmic and polarization resistances can be obtained by fitting the curve with an equivalent circuit, similar to that in our previous work [7]. The OCV, ohmic and polarization resistances of the fuel cell under each testing condition are listed in Table 1. The ohmic resistance of the cell showed very similar values in flowing air and oxygen, ranging from 0.08 to 0.16 Ω cm^2 when the testing temperature decreased from 700 to 600 °C. The polarization resistance of the fuel cell was much smaller under flowing oxygen, as compared to flowing air. The difference in polarization resistance between flowing oxygen and air is possibly related to the cathode reaction, especially to the diffusion of oxygen to the reaction site (see Fig. 3 and Table 1).

The power density of the cell in this study is higher than most of the reported values [14,15,23–25] and is comparable to those of Ahn's and Yang's [11–13]. Ahn showed a maximum power density of 1.95 W cm^{-2} at 0.32 V and 650 °C on a bi-layer GDC/ESB electrolyte, with H$_2$ at the anode and air at the cathode. Yang also showed a peak power density of 1.2 W cm^{-2} at 0.7 V and 650 °C on a bi-layer SDC-ScSZ electrolyte, using humidified H$_2$ and air at the anode and cathode, respectively. While the current results in air are a little lower than Ahn et al., the results under flowing oxygen are comparable to their results. Fig. 4 shows the calculated I–V curve at 650 °C in flowing oxygen, assuming a constant overall resistance over the entire current density range. A maximum power density of over 2 W cm^{-2} could be achieved under this condition. The high power density of the cell in this study is mainly attributed to the

Table 1
OCV, ohmic, and polarization resistance values of the fuel cell with air and oxygen supplied to the cathode at different temperatures.

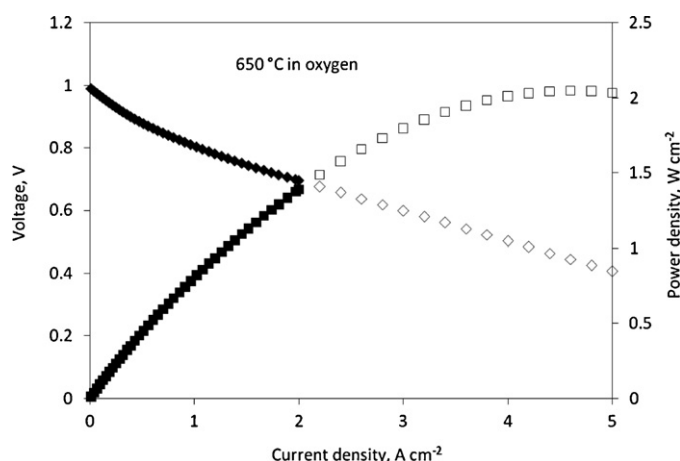|	OCV (V)		Ohmic resistance (Ω cm^2)		Polarization resistance (Ω cm^2)	
	Air	O$_2$	Air	O$_2$	Air	O$_2$
700 °C	0.94	0.98	0.08	0.09	0.09	0.02
650 °C	0.95	0.99	0.11	0.12	0.20	0.08
600 °C	0.99	1.00	0.16	0.16	0.39	0.26

Fig. 4. Predicted peak power density at 650 °C in oxygen with solid symbols representing experimental data and open symbols representing model calculations.

low ohmic resistance of the thin YSZ electrolyte. The ohmic resistance of the fuel cell in this study is lower than that of the fuel cell in our previous study, which had a very similar configuration, but a thicker YSZ layer of 8 μm. The fuel cell with 8 μm electrolyte had an ohmic resistance of 0.13, 0.17, and 0.27 Ω cm^2 at 700, 650, and 600 °C, respectively, while the corresponding values in this study were 0.08, 0.11, and 0.16 Ω cm^2, respectively. However, the ohmic resistance is still higher than that of the fuel cell with GDC/ESB electrolyte, which only registered 0.046 Ω cm^2 at 650 °C, but with a lower OCV of 0.77 V [11].

Although very high cell performance is demonstrated, the mechanical and electrical stability of the thin electrolyte is yet to be addressed. For this reason, the cell with the SDC-YSZ electrolyte was tested in flowing oxygen under a current density of 1 A cm^{-2} at 650 °C for more than 400 h. Fig. 5 shows the voltage of the cell as a function of operating time. The voltage of the cell only exhibited a slight decrease over 400 h, indicating high stability in cell performance. An SEM image of the cross-section of the fuel cell showed that the bi-layer electrolyte retained its mechanical integrity through the 400-h cell test. No micro-cracking in the electrolyte or delamination between the electrolyte and electrode was observed. Inter-diffusion between the YSZ and SDC was minimal, as was evident from the clear interface and from EDS analysis of the two layers (not shown in the figure). The high stability in cell performance can be attributed to the high mechanical and chemical stability of the bi-layer electrolyte and to the reduced operating temperature at which lower degradation rates are expected for the electrodes. This initial stability test suggests
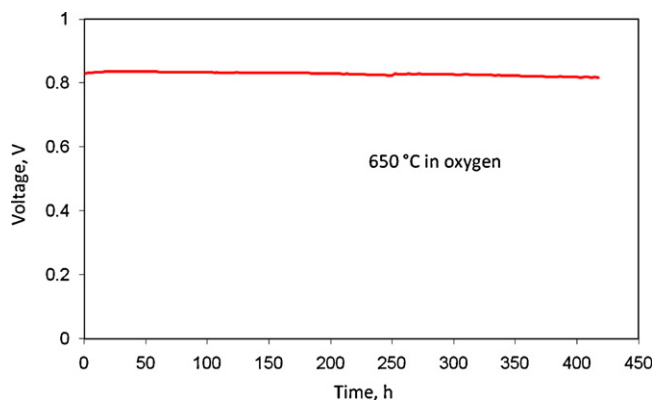
the feasibility of using a thin bi-layer electrolyte at intermediate temperatures.

4. Conclusions

A uniform and pore-free YSZ-SDC bi-layer electrolyte was fabricated by PLD on the anode substrate at 1000 °C. The bi-layer electrolyte had thicknesses of about 0.5 and 5 μm for YSZ and SDC, respectively. Fuel cells with the bi-layer electrolytes had OCVs of 0.94–1.00 V at 600–700 °C, higher than that of cells with single-layer SDC electrolytes. This indicates the effectiveness of the YSZ layer in blocking leakage current through the electrolyte. Power densities of 0.4–1 W cm^{-2} at 0.7 V were achieved in air at temperatures ranging from 600 to 700 °C. A peak power density of over 2 W cm^{-2} was estimated for the cell 650 °C in flowing oxygen, assuming a constant resistance over the entire range of current density. The very high cell performance is attributed to the low ohmic resistance of the cell, owing to the thin YSZ layer. More importantly, stability of the cell with the thin electrolyte was demonstrated throughout 400 h of cell testing. The voltage of the cell at a constant current density of 1 A cm^{-2} at 650 °C in flowing oxygen showed only a very slight change over the 400-h duration. SEM analysis of the cell after the 400 h test showed that the electrolyte had retained its microstructural integrity. The high cell performance and stability shows promise for operating solid oxide fuel cells at reduced temperatures. However, pulse laser deposition is a process with disadvantages of high production cost, slow deposition speed, and difficulty in large-scale production. Therefore, cost-effective approaches must be developed to fabricate the fuel cell with bi-layer electrolyte to make it commercially viable.

Acknowledgements

References

[1] B.C.H. Steele, Solid State Ionics 129 (2000) 95.
[2] T. Ishihara, H. Matsuda, Y. Takita, J. Am. Chem. Soc. 116 (1994) 3801.
[3] V. Dusastre, J. Kilner, Solid State Ionics 126 (1999) 163.
[4] E. Murray, M. Sever, S. Barnett, Solid State Ionics 148 (2002) 27.
[5] W. Wang, M. Mogensen, Solid State Ionics 176 (2005) 457.
[6] J. Stevenson, T. Armstrong, R. Carneim, L. Pederson, W. Weber, J. Electrochem. Soc. 143 (1996) 2772.
[7] Z. Lu, J. Hardy, J. Templeton, J. Stevenson, J. Power Sources 198 (2012) 90.
[8] T. Nguyen, T. Kato, K. Nozaki, T. Honda, A. Negishi, K. Kato, Y. Iimura, J. Electrochem. Soc. 153 (2006) A1310.
[9] Z. Lu, X. Zhou, J. Templeton, J. Stevenson, J. Electrochem. Soc. 157 (2010) B964.
[10] Z. Lu, X. Zhou, D. Fisher, J. Templeton, J. Stevenson, N. Wu, A. Ignatiev, Electrochem. Commun. 12 (2010) 179.
[11] J. Ahn, D. Pergolesi, M. Camaratta, H. Yoon, B. Lee, K. Lee, D. Jung, E. Traversa, E. Wachsman, Electrochem. Commun. 11 (2009) 1504.
[12] E. Wachsman, K. Lee, Science 334 (2011) 935.
[13] D. Yang, X. Zhang, S. Nikumb, C. Decès-Petit, R. Hui, R. Maric, D. Ghosh, J. Power Sources 164 (2007) 182.
[14] X. Zhang, M. Robertson, C. Decès-Petit, Y. Xie, R. Hui, W. Qu, O. Kesler, R. Maric, D. Ghosh, J. Power Sources 175 (2008) 800.
[15] Y. Leng, S. Chan, Electrochem. Solid-State Lett. 9 (2006) A56.
[16] M. Price, J. Dong, X. Gu, S. Speakman, E. Payzant, J. Am. Ceram. Soc. 88 (2005) 1812.
[17] T. Nguyen, K. Kobayashi, T. Honda, Y. Iimura, K. Kato, A. Negishi, K. Nozaki, F. Tappero, K. Sasaki, H. Shirahama, K. Ota, M. Dokiya, T. Kato, Solid State Ionics 174 (2004) 163.
[18] T. Tsai, E. Perry, S. Barnett, J. Electrochem. Soc. 144 (1997) L130.

Fig. 5. Stability of cell performance at 650 °C in oxygen over 400 h.

[19] B. Timurkutluk, C. Timurkutluk, M. Mat, Y. Kaplan, J. Power Sources 196 (2011) 9361.
[20] M. Matsuda, T. Hosomi, K. Murata, T. Fukui, M. Miyake, J. Power Sources 165 (2007) 102.
[21] S. Simner, M. Anderson, L. Pederson, J. Stevenson, J. Electrochem. Soc. 152 (2005) A1851.
[22] X. Chen, N.J. Wu, D.L. Ritums, A. Ignatiev, Thin Solid Films 342 (1999) 61.
[23] C. Xia, M. Liu, Solid State Ionics 144 (2001) 249.
[24] Y. Zhen, A. Tok, S. Jiang, F. Boey, J. Power Sources 178 (2008) 69.
[25] C. Ding, H. Lin, K. Sato, K. Amezawa, T. Kawada, J. Mizusaki, T. Hashida, J. Power Sources 195 (2010) 5487.
[26] J. Ahn, H. Yoon, K. Lee, M. Camaratta, E. Wachsman, Fuel Cells 9 (2009) 643.